Scientific Reports

https://doi.org/10.1038/s41598-026-38015-7

Article in Press

Nonlinear model reduction for large-scale structures via dual substructuring

Received: 14 September 2025

Accepted: 28 January 2026

Published online: 16 February 2026

Cite this article as: Flores P.A. Nonlinear model reduction for large-scale structures via dual substructuring. *Sci Rep* (2026). https://doi.org/10.1038/s41598-026-38015-7

Pedro A. Flores

Nonlinear Model Reduction for Large-Scale Structures via Dual Substructuring

Pedro A. Flores[1,*]

[1]Pontifical Catholic University of Peru, Applied Mechanics, Machines and Mechanisms Group, Lima, 15088, Peru

ABSTRACT

This work presents a nonlinear model reduction strategy for large-scale structural systems with localized nonlinearities based on a dual substructuring approach. The method combines the computational benefits of the dual Craig-Bampton formulation with the accuracy of nonlinear normal modes (NNMs) embedded within each substructure dynamic reduction. Internal nonlinearities are treated locally via invariant manifold-based approximations, while interface compatibility is enforced through interface forces, maintaining the modularity and flexibility of the dual formulation. The performance of the proposed method is assessed on a steel frame with localized nonlinearities subjected to harmonic loading. The results obtained with the proposed formulation were compared with those of the full finite element model. In both analyses, the Hilber–Hughes–Taylor (HHT) algorithm was employed as the time integration strategy. The reduced models achieve significant reductions in computational cost while preserving high accuracy in the predicted transient response. The approach demonstrates strong potential for efficient nonlinear dynamic simulation of complex engineering structures with localized nonlinearities.

1 Introduction

Dynamic analysis using the finite element method is essential in many engineering fields - including, but not limited to, mechanical, aerospace, and civil engineering - when dealing with systems that have a large number of degrees of freedom. However, such analyses are often limited by the substantial computational resources required to obtain time-domain responses of the structures under study. To address this challenge, model order reduction techniques have been developed. These reduction techniques operate directly on the governing equations of motion, which are often derived from a finite element discretization but are not limited to it. Depending on the specific formulation, some methods retain a subset of the original physical degrees of freedom while others rely entirely on a transformation to a new set of generalized coordinates. In all cases, the dimension of the reduced system is considerably smaller than that of the full model, yet it remains capable of accurately capturing the essential dynamic behavior of the structure, thus achieving substantial computational savings. Nevertheless, this reduction process can lead to a loss of accuracy compared to the original high-fidelity finite element model. As a result, a wide range of model reduction strategies have been studied over the past decades to balance computational efficiency with solution accuracy.

Among the various model reduction techniques developed, those based on substructuring divide the full system into smaller subsystems, each of which can be reduced individually before reassembling the complete structure. A key advantage of these methods is that they allow model reduction to be applied only to the substructures of interest, without requiring a full-system analysis to determine a global reduction strategy. The works of [1] and [2] introduced a method for reducing degrees of freedom through static condensation. Later, [3] proposed the component mode synthesis method, which uses the vibration modes of each substructure as the basis for model reduction. [4] later refined the method by introducing an incomplete set of free-interface normal modes, which were augmented with a correction term accounting for the contribution of the neglected modes. Similarly, [5] proposed an exact dynamic condensation method applicable to substructures, in which the accuracy of the approach does not depend on the selection of the master degrees of freedom - except in cases where the energy of the system has no contribution associated with the chosen master set. [6] later introduced a generalized method for coupling substructures in systems with non-classical damping, that is, without assuming proportional damping. [7] introduced an approach for damping synthesis using complex modes instead of real modes within substructures. [8] extended Rubin's method to more general damped systems. The generalization was achieved using residual flexibility modes, rigid-body modes represented in state-space form, and complex vibration modes. [9] introduced a new implementation technique for substructuring based on floating reference frames located near the centers of the bodies. [10] introduced a dual formulation of the classical Craig-Bampton method, based on free-interface vibration modes and residual flexibility components, in which substructures are assembled through interaction forces that enforce only weak compatibility across interfaces, resulting in reduced matrices with improved computational efficiency. Later, [11] extended the dual Craig-Bampton method to include dynamically non-classically damped systems, using residual flexibility modes and rigid-body modes represented in state-space form, similarly to the approach taken by [8].

The methods discussed thus far are primarily developed for the order reduction of linear systems, with only a subset of them explicitly addressing non-classically damped configurations. However, these methods do not inherently include nonlinear terms and therefore cannot directly capture nonlinear behavior. This limitation has also been investigated, and several model-order reduction techniques have been proposed to address such nonlinearities. Nonlinear normal modes (NNMs) were first introduced by [12] and later formalized by [13], who proposed their use as a basis for model order reduction in analogy with the classical modal expansion theorem. When it comes to their computation, the deterministic approach proposed by [13] relies on the invariant manifold theorem to determine the coefficients defining the NNMs. More recently, [14],[15] and [16] have developed a theoretical framework in which they are computed as subspectral submanifolds. Building on these concepts, for example, [17] extended the Craig–Bampton component mode synthesis method to *N*-degree-of-freedom systems with nonlinearities by incorporating NNMs. They emphasized that, although the method achieves a significant reduction in the number of degrees of freedom for each substructure, the computation of NNMs becomes computationally demanding when the number of degrees of freedom exceeds one. Moreover, the formulation is derived under the assumption of undamped dynamics, thereby neglecting the influence of damping effects during the construction of the reduced-order model. [18] used NNMs based on the invariant manifold theorem to develop a technique that incorporates energy dissipation due to friction in assembled structures with frictional interfaces, but still uses proportional damping during the model reduction. [19] used the reduction via subspectral submanifolds to perform Montecarlo simulations in nonlinear dynamical systems, but once again, only proportional damping is considered.

Other approaches to nonlinear model order reduction that do not use NNMs have also been developed. [20] addressed assemblies with contact interfaces by applying the dual Craig–Bampton method in the frequency domain, exploiting spectral orthogonality of mode sets and retaining interface forces as generalised coordinates to achieve spatial and temporal reduction in structures with localized nonlinearities. Nevertheless, as it is based on the classic dual Craig-Bampton method, it is not possible for it to consider a case of general damping. [21] further extended the concept of substructuring to systems with localised nonlinearities by formulating the coupling procedure entirely in the modal domain. In their formulation, each linear substructure is represented through a truncated set of vibration modes obtained from its finite element model, while the nonlinear components—typically located at the interfaces—are retained in their physical coordinates. The coupling between substructures is then enforced through modal compatibility and equilibrium conditions, allowing the nonlinear forces to act as coupling terms between the reduced modal coordinates. This approach effectively decouples the reduction of linear substructures from the treatment of nonlinear connections, which significantly improves computational efficiency and flexibility compared to traditional approaches that require global linearisation. The authors validated their method on several case studies, including systems with nonlinear joints and contact interfaces, demonstrating that the proposed formulation preserves the accuracy of the full-order finite element model while achieving substantial reductions in computational cost. The study also highlighted the versatility of the modal-domain framework for handling different types of nonlinearities and for integrating experimental or reduced-order models of substructures within the same computational framework. However, damping is not considered in the development of the reduction method. More recently, [22] advanced nonlinear substructuring techniques by formulating the coupling procedure in the frequency domain. In their approach, the global system is decomposed into linear substructures connected through nonlinear interface elements, allowing the nonlinear behaviour to be efficiently captured without resorting to full time-domain simulations. By employing a spectral-based coupling scheme, the method accurately reproduces the frequency-response characteristics of high-fidelity models while considerably reducing computational cost. Collectively, these developments mark a progressive shift from linear reduction techniques toward more generalised substructuring methods capable of accommodating localised nonlinearity and frequency-domain coupling. However, the method does not account for nonlinearities within the individual substructures, as nonlinear effects are considered exclusively at the interface elements.

As can be inferred from the previous discussion, while several model order reduction techniques have been proposed to account for nonlinear effects—some of them explicitly relying on the concept of nonlinear normal modes—the majority of these approaches either neglect damping altogether during the reduction process or incorporate it under restrictive assumptions. In most existing formulations, damping is introduced in a simplified manner, for instance through block-diagonal damping matrices or by considering dissipation mechanisms solely associated with contact or frictional interfaces. As a result, the effects of general, and in particular non-proportional, damping are not consistently retained throughout the reduction procedure. For example, although the approach proposed by [21] includes damping terms, their influence on the construction of the reduced-order basis remains limited, whereas the formulation presented in [20] relies on a classical Craig–Bampton framework in which damping effects are either neglected or introduced only after the reduction stage. These observations motivate the development of a reduction framework in which general damping is explicitly preserved in the equations of motion and actively contributes to the reduced-order dynamics, particularly within a dual Craig–Bampton formulation.

This work presents a substructuring method based on the dual Craig–Bampton approach for non-classically damped systems, in which nonlinear normal modes are employed to enhance the dynamic component of the reduced-order approximation. First, the equations of motion of a system discretized by the finite element method are formulated in state-space form, with the aim of approximating its response as the superposition of a static and a dynamic component. The dynamic component of the approximation is then analyzed in detail, showing how nonlinear normal modes—formulated according to the methodology proposed in [13]—are incorporated to represent the vibratory behavior of the system. Subsequently, the static component of the approximation is addressed, and the complete formulation of the proposed method is established. Finally, to validate the effectiveness of the methodology, a case study is presented involving an industrial building structure subjected to harmonic loads, with localized cubic nonlinearities, proportional and non-proportional damping.

2 Proposed Substructuring Method

This methodology presents an extension of the Craig-Bampton substructuring method for nonlinear systems with localized nonlinearities by integrating NNMs within a dual Craig-Bampton framework. Consider the following discretized system using the finite element method:

$$\mathbf{M}\ddot{\mathbf{u}} + \mathbf{C}\dot{\mathbf{u}} + \mathbf{K}\mathbf{u} = \mathbf{f} \tag{1}$$

Where $\mathbf{M}$ denotes the mass matrix, $\mathbf{C}$ the damping matrix, $\mathbf{K}$ the stiffness matrix, $\mathbf{u}$ the vector of nodal displacements, and $\mathbf{f}$ the vector of external forces. The system is partitioned into N substructures, each of which has the following equation of motion:

$$\mathbf{M}^{(s)}\ddot{\mathbf{u}}^{(s)} + \mathbf{C}^{(s)}\dot{\mathbf{u}}^{(s)} + \mathbf{K}^{(s)}\mathbf{u}^{(s)} = \mathbf{f}_b^{(s)} + \mathbf{f}_i^{(s)} \tag{2}$$

Where $\mathbf{f}_b$ is the vector containing the forces at the interface where the substructure has been separated from the rest of the system, $\mathbf{f}_i$ is the vector containing the forces within the substructure, and the superscript (s) indicates that each term in the equation corresponds to substructure $s = 1, 2, \ldots, N$. It is important to note at this point that matrix $\mathbf{C}$ does not need to be proportional to either the mass or the stiffness of the system. This means that the system is, in general, non-classically damped, which implies that matrix $\mathbf{C}$ cannot be diagonalized using the linear complex modal matrix Ω.

Some of the forces acting both within the interior and at the boundaries of the substructures may be nonlinear in nature, and are therefore denoted as $\mathbf{f}_{NL}$. The nonlinear nature of these forces is assumed to be directly proportional to some power of the nodal displacements or velocities. Thus:

$$\mathbf{f}_{NL}^{(s)} = \sum_{i=1}^{n} \mathbf{K}_i^{(s)} \mathbf{u}^{n^{(s)}} + \sum_{j=1}^{p} \mathbf{K}_j^{(s)} \dot{\mathbf{u}}^{p^{(s)}} \tag{3}$$

Where $\mathbf{K}_i^{(s)}$ and $\mathbf{K}_j^{(s)}$ represent matrices that contain the coefficients of the nonlinear terms. With this consideration, the forces acting on the substructure can be expressed as:

$$\mathbf{M}^{(s)}\ddot{\mathbf{u}}^{(s)} + \mathbf{C}^{(s)}\dot{\mathbf{u}}^{(s)} + \mathbf{K}^{(s)}\mathbf{u}^{(s)} = \mathbf{f}_{b_L}^{(s)} + \mathbf{f}_{i_L}^{(s)} + \mathbf{f}_{NL}^{(s)} \tag{4}$$

Where $\mathbf{f}_{b_L}^{(s)}$ and $\mathbf{f}_{i_L}^{(s)}$ are, respectively, the boundary and internal forces of the substructure with linear characteristics. To carry out the model order reduction, the equation of motion is first expressed in state-space form, which yields:

$$\mathbf{A}^{(s)}\dot{\mathbf{z}}^{(s)} + \mathbf{B}^{(s)}\mathbf{z}^{(s)} = \mathbf{Q}^{(s)} \tag{5}$$

Where:

$$\mathbf{A}^{(s)} = \begin{bmatrix} \mathbf{C}^{(s)} & \mathbf{M}^{(s)} \\ \mathbf{M}^{(s)} & \mathbf{0} \end{bmatrix}, \mathbf{B}^{(s)} = \begin{bmatrix} \mathbf{K}^{(s)} & \mathbf{0} \\ \mathbf{0} & -\mathbf{M}^{(s)} \end{bmatrix}, \mathbf{Q}^{(s)} = \begin{bmatrix} \mathbf{f}_{b_L}^{(s)} + \mathbf{f}_{i_L}^{(s)} \\ \mathbf{0} \end{bmatrix} + \begin{bmatrix} \mathbf{f}_{NL}^{(s)} \\ \mathbf{0} \end{bmatrix} \tag{6}$$

As in the dual Craig-Bampton method developed by [11], the vector $\mathbf{z}^{(s)}$ will be approximated by a static part and a dynamic part.

$$\mathbf{z}^{(s)} \approx \mathbf{z}_{sta}^{(s)} + \mathbf{z}_{dyn}^{(s)} \tag{7}$$

2.1 Dynamic part of the approximation

To approximate the dynamic part of the system's response, nonlinear normal modes will be employed. The procedure described by [13] will be used to compute their coefficients. Each nonlinear normal mode is approximated as a power series up to the highest order present in the polynomials describing the nonlinear forces in the substructure. Equation 5 can be rewritten as:

$$\dot{\mathbf{z}} = -\mathbf{A}^{(s)^{-1}}\mathbf{B}^{(s)}\mathbf{z}^{(s)} + \mathbf{A}^{(s)^{-1}}\mathbf{Q}^{(s)}_{NL} = \mathbf{f}^{(s)}(\mathbf{z}) = \begin{bmatrix} f_1^{(s)} \\ f_2^{(s)} \\ \vdots \\ f_{2N_s}^{(s)} \end{bmatrix} \tag{8}$$

With N_s being the total number of degrees of freedom of the substructure, including the ones at the interface, and:

$$\mathbf{Q}^{(s)}_{NL} = \begin{bmatrix} \mathbf{f}^{(s)}_{NL} \\ \mathbf{0} \end{bmatrix} \tag{9}$$

In analogy with the dual Craig–Bampton method [11], where external (purely linear) forces are not included in the computation of normal modes, such forces are also disregarded in this work. However, unlike the original formulation, the nonlinear forces must be retained at this stage to determine the coefficients of the nonlinear normal modes. To proceed with the approximation, only the vibration modes associated with the displacements and velocities of the nodes at the substructure boundaries will be taken into account. Let u_j denote the displacement of an interface node in a given degree of freedom, and v_j its associated velocity in that same degree of freedom, where $j = 1, \ldots, n_b$. Each displacement u_i and its corresponding velocity v_i within the substructure, with $i = 1, \ldots, N_s$, $i \neq j$, are expressed as functions of u_j and v_j.

$$\begin{aligned} u_i = {} & a_{1i}u_j + a_{2i}v_j + a_{3i}u_j^2 + a_{4i}u_jv_j + a_{5i}v_j^2 + a_{6i}u_j^3 \\ & + a_{7i}u_j^2 + a_{8i}u_jv_j^2 + a_{9i}v_j^3 \end{aligned} \tag{10}$$

$$\begin{aligned} v_i = {} & b_{1i}u_j + b_{2i}v_j + b_{3i}u_j^2 + b_{4i}u_jv_j + b_{5i}v_j^2 + b_{6i}u_j^3 \\ & + b_{7i}u_j^2 + b_{8i}u_jv_j^2 + b_{9i}v_j^3 \end{aligned} \tag{11}$$

The j-th nonlinear normal mode $\mathbf{m}_j$ is determined by constructing an invariant manifold that is parameterized in terms of u_j and v_j. In this work, the parameterization is carried out using a polynomial expansion up to third order, which allows the capture of quadratic and cubic nonlinear effects. Nevertheless, the same procedure can be extended to higher-order terms if required, depending on the complexity and strength of the nonlinearities present in the substructure.

$$\mathbf{m}_j = \mathbf{m}_j(u_j, v_j) = \begin{bmatrix} \mathbf{m}_{0_j} + \mathbf{m}_{1_j}(u_j, v_j) + \mathbf{m}_{2_j}(u_j^2, v_j^2) \end{bmatrix} \begin{Bmatrix} u_j \\ v_j \end{Bmatrix} \tag{12}$$

With:

$$\mathbf{m}^0{}_j = \begin{bmatrix} a_{11} & a_{21} \\ b_{11} & b_{21} \\ \vdots & \vdots \\ a_{1j-1} & a_{2j-1} \\ b_{1j-1} & b_{2j-1} \\ 1 & 0 \\ 0 & 1 \\ a_{1j+1} & a_{2j+1} \\ b_{1j+1} & b_{2j+1} \\ \vdots & \vdots \\ a_{12N_s} & a_{22N_s} \\ b_{12N_s} & b_{22N_s} \end{bmatrix}$$

$$\mathbf{m}_{1_j}(u_j, v_j) = \begin{bmatrix} a_{31}u_j + a_{41}v_j & a_{51}v_j \\ b_{31}u_j + b_{41}v_j & b_{51}v_j \\ \vdots & \vdots \\ a_{3\,j-1}u_j + a_{4\,j-1}v_j & a_{5\,j-1}v_j \\ b_{3\,j-1}u_j + b_{4\,j-1}v_j & b_{5\,j-1}v_j \\ 0 & 0 \\ 0 & 0 \\ a_{3\,j+1}u_j + a_{4\,j+1}v_j & a_{5\,j+1}v_j \\ b_{3\,j+1}u_j + b_{4\,j+1}v_j & b_{5\,j+1}v_j \\ \vdots & \vdots \\ a_{32N_s}u_j + a_{42N_s}v_j & a_{52N_s}v_j \\ b_{32N_s}u_j + b_{42N_s}v_j & b_{52N_s}v_j \end{bmatrix} \tag{13}$$

$$\mathbf{m}_{2_j}(u_j, v_j) = \begin{bmatrix} a_{61}u_j^2 + a_{81}v_j^2 & a_{71}u_j^2 + a_{91}v_j^2 \\ b_{61}u_j^2 + b_{81}v_j^2 & b_{71}u_j^2 + b_{91}v_j^2 \\ \vdots & \vdots \\ a_{6\,j-1}u_j^2 + a_{8\,j-1}v_j^2 & a_{7\,j-1}u_j^2 + a_{9\,j-1}v_j^2 \\ b_{6\,j-1}u_j^2 + b_{8\,j-1}v_j^2 & b_{7\,j-1}u_j^2 + b_{9\,j-1}v_j^2 \\ 0 & 0 \\ 0 & 0 \\ a_{6\,j+1}u_j^2 + a_{8\,j+1}v_j^2 & a_{7\,j+1}u_j^2 + a_{9\,j+1}v_j^2 \\ b_{6\,j+1}u_j^2 + b_{8\,j+1}v_j^2 & b_{7\,j+1}u_j^2 + b_{9\,j+1}v_j^2 \\ \vdots & \vdots \\ a_{62N_s}u_j^2 + a_{82N_s}v_j^2 & a_{72N_s}u_j^2 + a_{92N_s}v_j^2 \\ b_{62N_s}u_j^2 + b_{82N_s}v_j^2 & b_{72N_s}u_j^2 + b_{92N_s}v_j^2 \end{bmatrix}$$

From the governing relations, it follows that $18N_s - 2$ equations must be solved to fully determine the parameterization of a nonlinear normal mode. These equations are built according to [13] using the functions $\mathbf{f}^{(s)}(\mathbf{z}^{(s)})$ defined in 8. These equations are the ones presented in 14 and 15.

$$v_i = \frac{\partial u_i}{\partial u_j} v_j + \frac{\partial u_i}{\partial v_j} f_j^{(s)} \tag{14}$$

$$f_i^{(s)} = \frac{\partial v_i}{\partial u_j} v_j + \frac{\partial v_i}{\partial v_j} f_j^{(s)} \tag{15}$$

The term $\mathbf{m}_{0_j}$ contains the linear contribution of the normal modes, while $\mathbf{m}_{1_j}$ and $\mathbf{m}_{2_j}$ account for the nonlinear contributions, here considered up to cubic order, although the series could be extended as required. At this point, it is important to note that the calculation of the coefficients must be carried out for each j nonlinear normal mode.

The restriction introduced in Sec. 2 is critical at this stage: the nonlinear forces must be expressible as power series in terms of the degrees of freedom of the interior nodes of the substructure. If this condition is not met, the equations for the nonlinear normal modes cannot be solved directly. For instance, geometric nonlinearities have been treated in some previous works [23, 24, 25]. The potential impact of such an approximation on the accuracy of the results and on the correct representation of the force throughout the time domain is outside the scope of this work. This formulation captures the nonlinearities in the system and, in some sense, parallels the superposition principle of the modal expansion theorem, where a complex dynamic system is represented as the sum of simpler subsystems [13].

In principle, a nonlinear normal mode can be computed for each degree of freedom at the n_b interface nodes of the substructure. However, doing so may require even more computational effort than solving the full dynamic problem. Therefore, as in the linear dual Craig-Bampton method, model order reduction remains practical only if a limited number of nonlinear normal modes are retained. The decision regarding how many modes to include, and which interface degrees of freedom to use for

parameterizing the invariant manifolds, is left to the discretion of the user. This decision becomes increasingly important as the number of degrees of freedom in the substructure grows.

Once r nonlinear normal modes have been selected, the dynamic component of the approximation can be expressed as:

$$\mathbf{z}_{dyn} = \{\mathbf{M}(\mathbf{w})\}\mathbf{w} \tag{16}$$

With

$$\mathbf{M}(\mathbf{w}) = [\mathbf{m}_{0_1}\ \mathbf{m}_{1_1}\ \mathbf{m}_{2_1} \ldots \mathbf{m}_{0_r}\ \mathbf{m}_{1_r}\ \mathbf{m}_{2_r}] \tag{17}$$

$\mathbf{w}$ denotes the modal vector that gathers the $2r$ degrees of freedom corresponding to the n_b interface nodes of the substructure chosen for the computation of the nonlinear normal modes. These degrees of freedom include both the displacements and velocities associated with the selected interface nodes, and they serve as the reduced set of coordinates that define the dynamic contribution of the system within the model order reduction framework. By focusing exclusively on these $2r$ coordinates, the method captures the essential nonlinear dynamic behavior while significantly reducing computational complexity. The modal vector $\mathbf{w}$ is given in equation 18.

$$\mathbf{w} = [u_1\ v_1\ u_2\ v_2\ \ldots\ u_r\ v_r]^T \tag{18}$$

As described by [13], the results obtained can be used to represent the nonlinear behavior of the dynamical system on an invariant, two-dimensional invariant manifold tangent at the equilibrium point to the linear normal mode eigenspace.

2.2 Static part of the approximation

In the linear dual Craig–Bampton method [11], the static component of the approximation accounts only for the interface forces, neglecting those acting within the interior of the substructure. This same approximation approach can be replicated in the proposed method, particularly because the effects of the nonlinearities have already been incorporated into the dynamic component of the formulation. Consequently, both the internal forces of the substructure and the nonlinear forces can be disregarded, resulting in static approximation equations that are identical to those of the original method.

To carry out the static approximation, the term $\mathbf{z}$, the internal forces within the substructure, and the forces of nonlinear nature are excluded from the equation of motion. Thus, the only forces remaining acting on the substructure are those at the interfaces.

$$\mathbf{B}^{(s)}\mathbf{z}^{(s)}_{sta} = \begin{Bmatrix} \mathbf{f}_b^{(s)} \\ \mathbf{0} \end{Bmatrix} = \begin{bmatrix} \mathbf{B}_{ss}^{(s)T}\boldsymbol{\lambda} \\ \mathbf{0} \end{bmatrix} \tag{19}$$

Here, $\mathbf{B}^{(s)}_{ss}$ denotes a Boolean matrix that enforces the compatibility conditions between the substructure interfaces and the remainder of the model, such that:

$$\sum_{i=1}^{N} \mathbf{B}^{(s)}_{ss}\mathbf{u}^{(s)} = \mathbf{0} \tag{20}$$

and $\boldsymbol{\lambda}$ represents the vector of all Lagrange multipliers. In the absence of rigid body modes in the substructure, the matrix $\mathbf{B}^{(s)}$ becomes invertible, and the static approximation can then be expressed as:

$$\mathbf{z}^{(s)}_{sta} = -\mathbf{B}^{(s)-1}\mathbf{B}^{(s)}_{ss}\boldsymbol{\lambda} \tag{21}$$

If the substructure contains rigid body modes, the state space elastic flexibility matrix $G^{(s)}_{ss}$ must be obtained using the inertia-relief projection matrix $\mathbf{P}^{(s)}_{ss}$, as defined in [8]:

$$\mathbf{P}^{(s)}_{ss} = \mathbf{I}^{(s)} - \mathbf{A}^{(s)}\mathbf{R}^{(s)}_{ss}\left(R^{(s)T}_{ss}\mathbf{A}^{(s)}R^{(s)}_{ss}\right)^{-1}R^{(s)T}_{ss} \tag{22}$$

along with any generalized inverse $\mathbf{B}^{(s)^+}$ of the matrix $\mathbf{B}^{(s)}$:

$$G^{(s)}_{ss} = \mathbf{P}^{(s)T}_{ss}\mathbf{B}^{(s)^+}\mathbf{P}^{(s)}_{ss} \tag{23}$$

Then, the static approximation is given by:

$$\mathbf{z}_{sta} = \begin{pmatrix} \mathbf{R}_{ss}^{(s)} - \mathbf{G}_{ss}^{(s)} \mathbf{B}_{(s)T} \end{pmatrix} \begin{bmatrix} \mathbf{u}^{1} \\ \alpha^{(s)} \\ \lambda \end{bmatrix} \tag{24}$$

It should be noted that when rigid body modes are absent, Eq. 24 simplifies to Eq. 21. The full approximation of the system's response can be expressed as:

$$\mathbf{z} \approx \mathbf{z}_{sta} + \mathbf{z}_{dyn} = \begin{pmatrix} \mathbf{R}_{ss}^{(s)} - \mathbf{G}_{ss}^{(s)} \mathbf{B}_{(s)T} \end{pmatrix} \begin{bmatrix} \mathbf{u}^{1} \\ \alpha^{(s)} \\ \lambda \end{bmatrix} + \{\mathbf{M}(\mathbf{w})\}\mathbf{w} \tag{25}$$

Unlike previous approaches that depend on modal derivatives or hyper-reduction strategies, the method developed here retains the dual Craig-Bampton formulation while incorporating NNMs at the substructure level. This ensures compatibility with systems exhibiting nonclassical damping and localized nonlinearities expressed as high-order polynomials.

3 Application example

This section presents an application example. The dynamic response was computed in two different ways: first, using the ANSYS software package, which applies the HHT method [26] for solving transient problems; and second, through the method proposed in this work, which involves substructuring, model order reduction, and reassembly of the equations of motion, subsequently solved using the same time integration scheme.

3.1 Case study: Industrial building subjected to sinusoidal loads with proportional damping

The proposed method was applied to analyze a steel structure representing an industrial building, in which the joints of the frames were modeled as nonlinear torsional springs. This structure was subjected to horizontal sinusoidal loads, and the aim of the simulation was to determine the time history of horizontal displacements at specific points. The mechanical properties of the structural material, the stiffness constant k of the nonlinear torsional spring (whose moment corresponds to a cubic nonlinearity in the rotation ϑ, expressed as $M = k\vartheta^3$), as well as the proportional damping coefficients α and β, are listed in Table 1. The geometry described above is illustrated in Figures 1, 2, and 3.

3.1.1 Characteristics of the model

The geometry of the model is based on a truss with the dimensions and layout depicted in Figure 1. This figure also indicates the direction and points of application of sinusoidal loads, together with the locations of both fixed and sliding joints within the structure.

Table 1. Building Geometry, Material Properties, and Damping Coefficients

Characteristic	Magnitude	Unit
Column height	8.5	m
Span between columns	20	m
Total frame height	10.5	m
Spacing between frames	6	m
Density	7850	$kg \cdot m^{-3}$
Young's modulus	2.1×10^5	MPa
Poisson's ratio	0.3	
k	10	$N \cdot m^{-3}$
α	1.25×10^{-3}	s^{-1}
β	2.5×10^{-3}	s

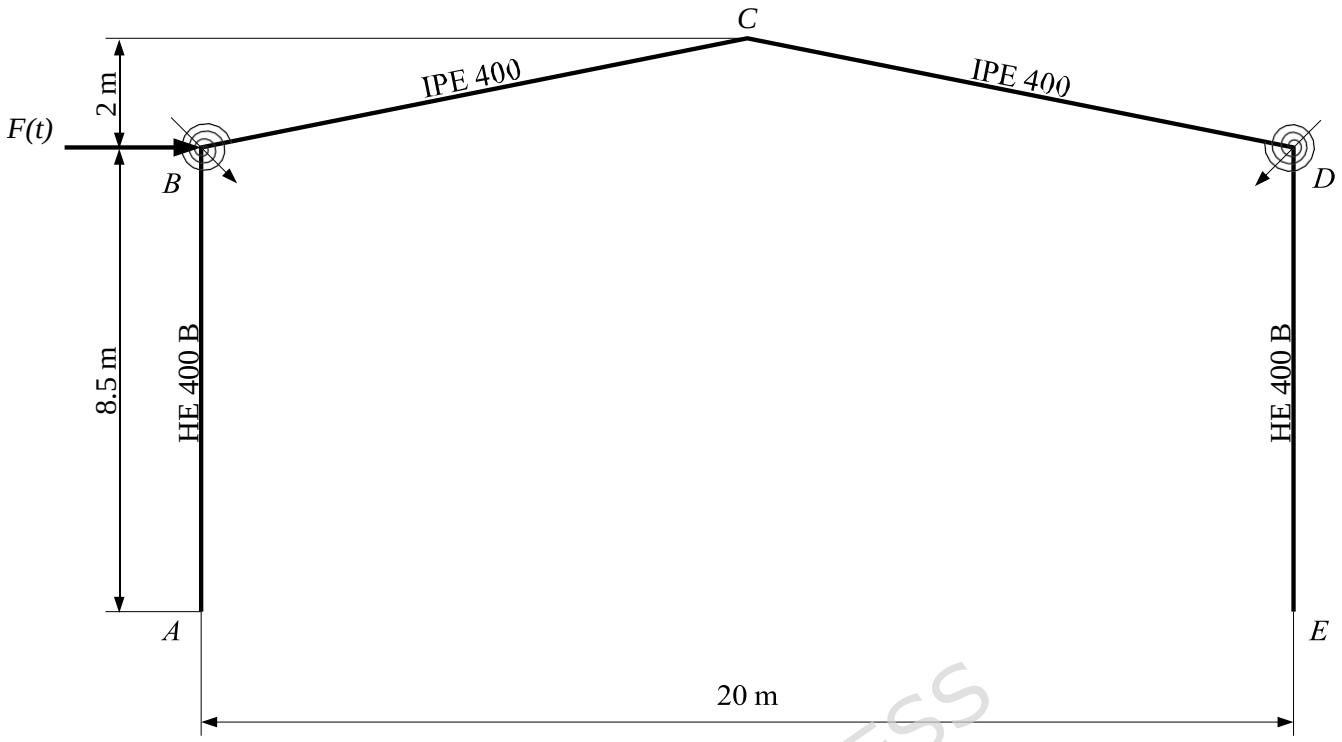

Figure 1. Front view of industrial building

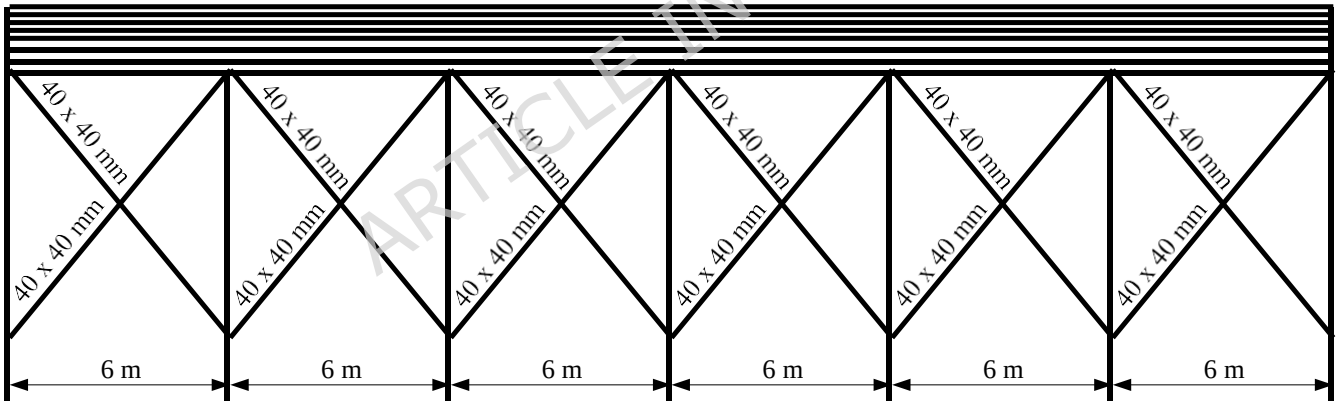

Figure 2. Lateral view of industrial building

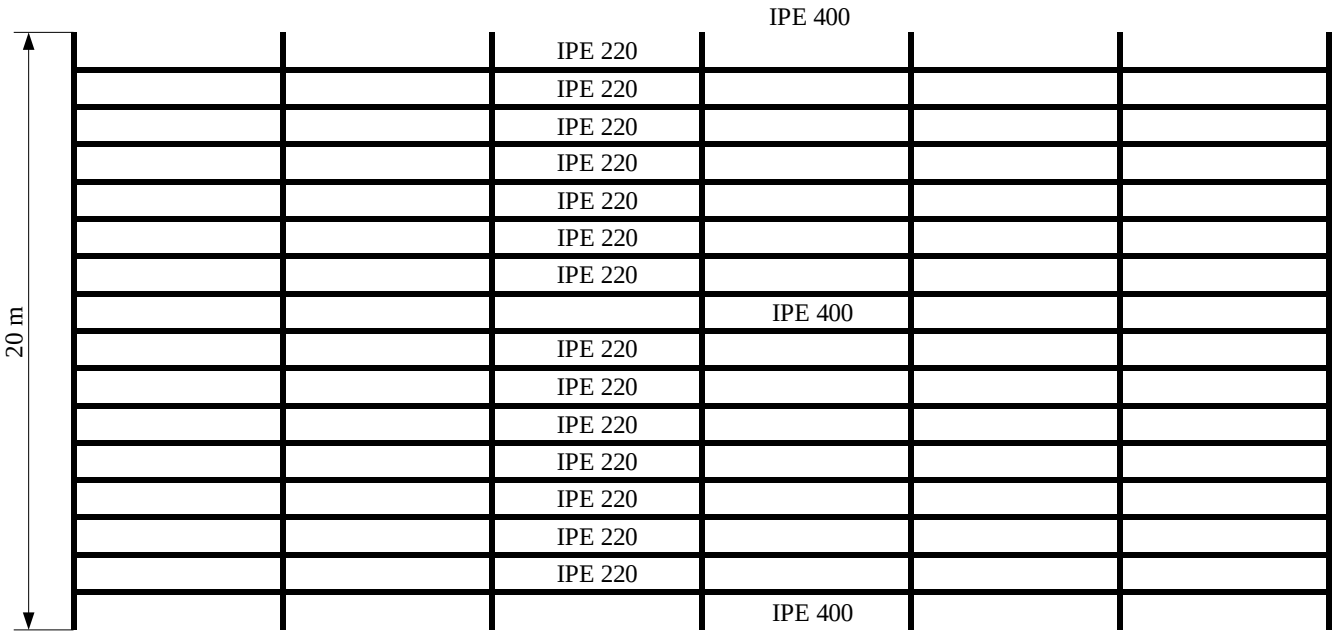

Figure 3. Lateral view of industrial building

3.1.2 Mesh

The meshing was carried out using three-node beam elements. In total, 22439 nodes and 11310 elements were used. It is important to note that these elements have six degrees of freedom per node: three translational degrees of freedom and three rotational degrees of freedom.

3.1.3 Load and boundary conditions

As shown in Figure 1, a horizontal lateral force was applied at the top end of the left column of each frame, defined as $F(t) = P\sin(\Omega\, t)$. The characteristics of this force are presented in Table 2. The frequency value $\Omega = 16.62\ \text{rad} \cdot \text{s}^{-1}$ was

Table 2. Characteristics of the applied load on the industrial building

Characteristic	Magnitude	Unit
Magnitude of force P	10^4	N
Frequency Ω	16.62	$\text{rad}\cdot\text{s}^{-1}$

obtained from a previous modal analysis, whose results are shown in Figure 4. This analysis reveals that the natural frequency most likely to be excited by lateral forces applied at the ends of the portal frame columns corresponds to the structure's second mode, with a frequency of 2.645 Hz ≈ 16.62 rad · s^{-1}.

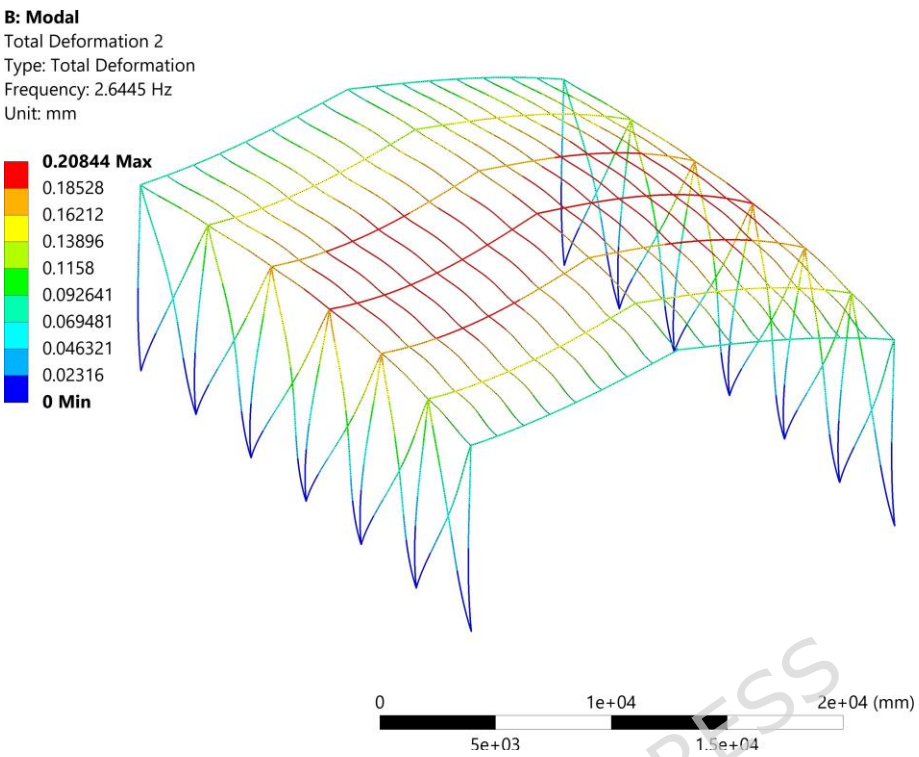

Figure 4. Mode of vibration at 16.62 rad · s^{-1}

3.1.4 Results using the HHT method

The equations of motion for the system are the following:

$$\mathbf{M}\ddot{\mathbf{u}} + \mathbf{C}\dot{\mathbf{u}} + \mathbf{K}\mathbf{u} + \mathbf{K}_{NL}\mathbf{u}(\varphi) = \mathbf{f}_0 \cos \Omega t \tag{26}$$

Where the matrix $\mathbf{K}_{NL}$ contains the coefficients k of the nonlinear springs, and the vector $\mathbf{u}(\varphi)$ contains the third-order terms of the rotation coordinates φ associated with the rotational degrees of freedom of the nonlinear springs in the model.

The initial time step for solving the equations of motion was set to $\Delta t = 0.01$ s, with the step size subsequently adjusted by ANSYS®'s built-in adaptive algorithm. The total simulation time required to solve the equations of motion, using the finite element discretization, was 293 s, and the process consumed 400 MB of RAM. Figure 5 presents the horizontal displacement of joint *B* in the central portal frame of the industrial building, obtained from a transient analysis performed with the HHT method.

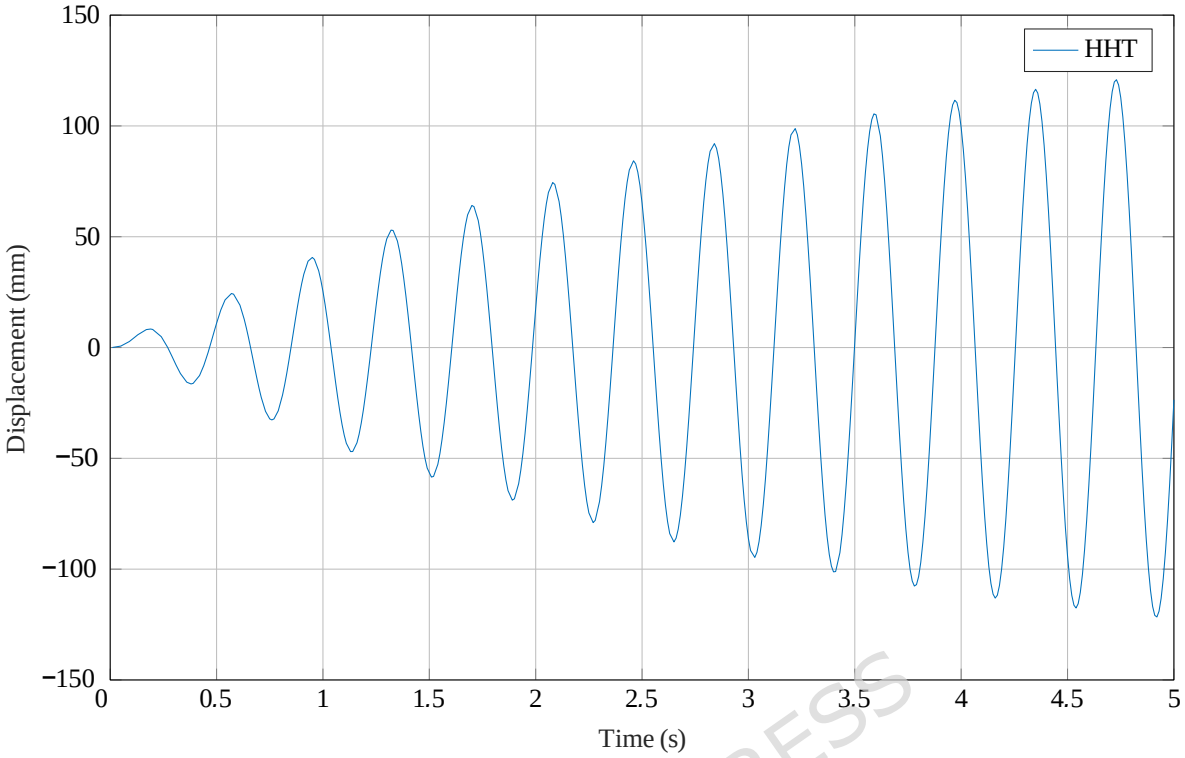

Figure 5. Horizontal displacement of node B of the central frame using HHT direct integration method

The forced response curve corresponding to joint *B* can be observed in Figure 6.

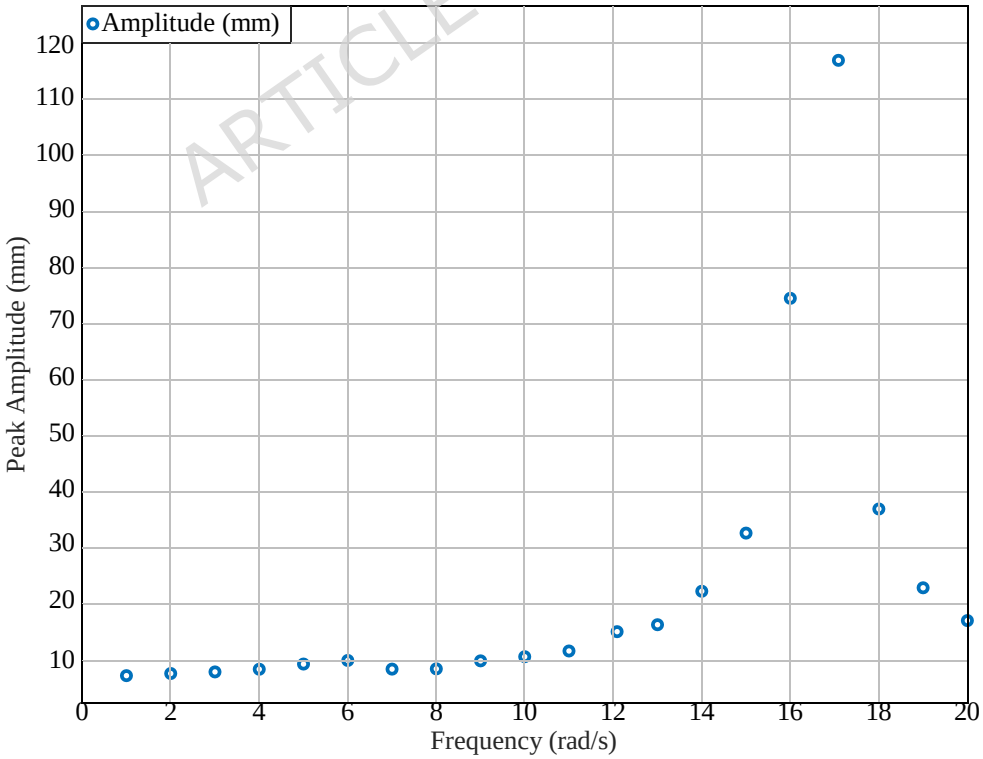

Figure 6. Forced response curve corresponding to joint *B*

3.1.5 Results Using the Implemented Substructuring Method

In this simulation, the efficiency of the substructuring method was demonstrated by taking advantage of the repetitive nature of identical substructures, which significantly reduced the computational time needed to compute the industrial building's response using the HHT method. The adopted approach involved extracting the intermediate frames of the structure as individual substructures, as illustrated in Figure 7. The resulting substructure is presented in Figure 8.

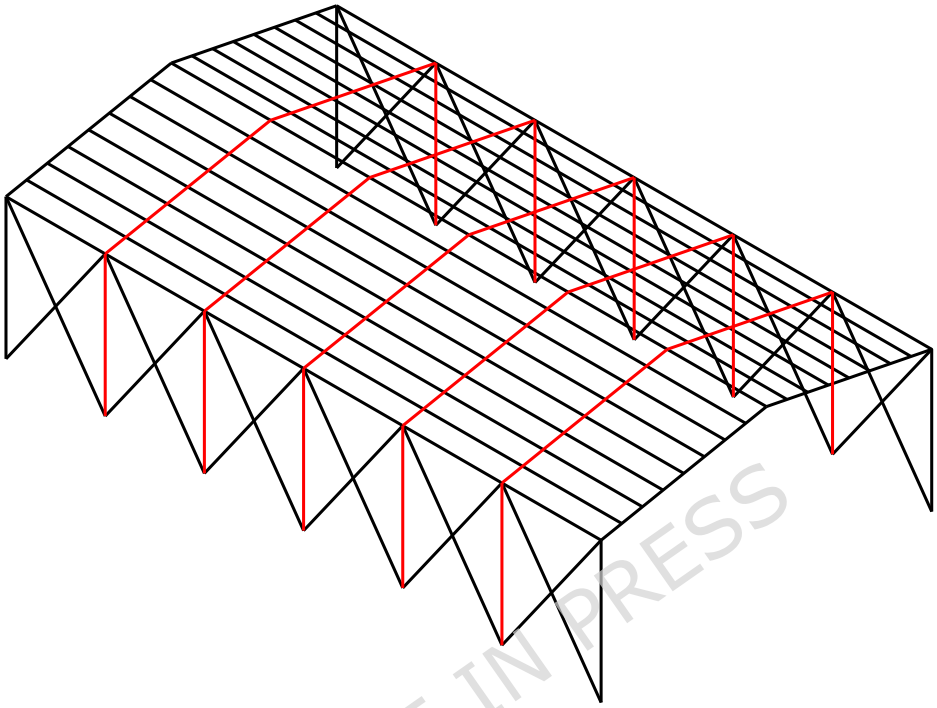

Figure 7. Substructuring strategy to be employed. The frames selected as substructures are highlighted in red.

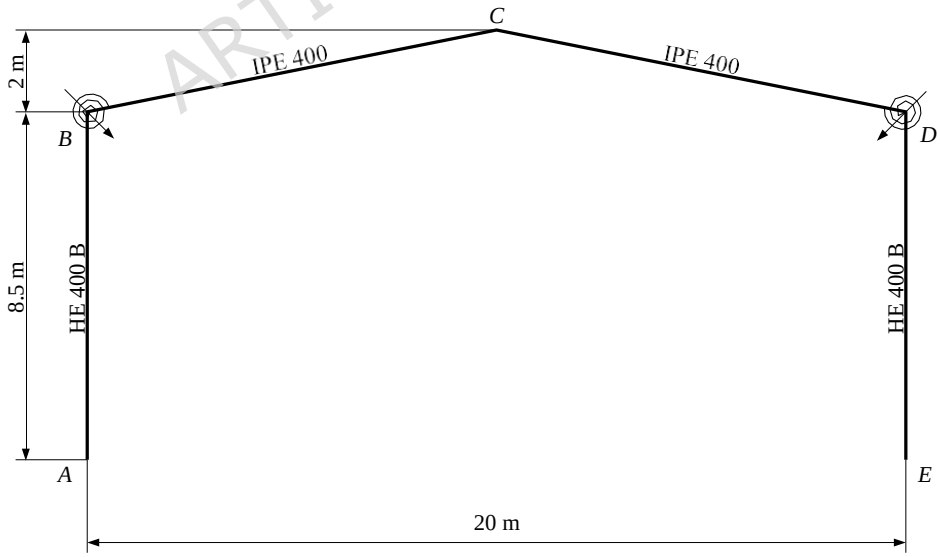

Figure 8. Frame substructure used for model order reduction.

The nonlinear normal modes were computed with respect to the translational and rotational degrees of freedom of nodes *B* and *D*, since the nonlinear torsional springs at these nodes primarily depend on the rotational degrees of freedom. The remainder of the building was considered as a separate substructure, as illustrated in Figure 9. Originally, each frame-type substructure

had 4,548 state-space coordinates, which were reduced to only 8 after model reduction. The state-space coordinates selected for the computation of the nonlinear normal modes were those corresponding to the horizontal displacements of nodes B and D, as well as the in-plane rotations of the same nodes. Consequently, a total of four nonlinear normal modes were computed for each frame.

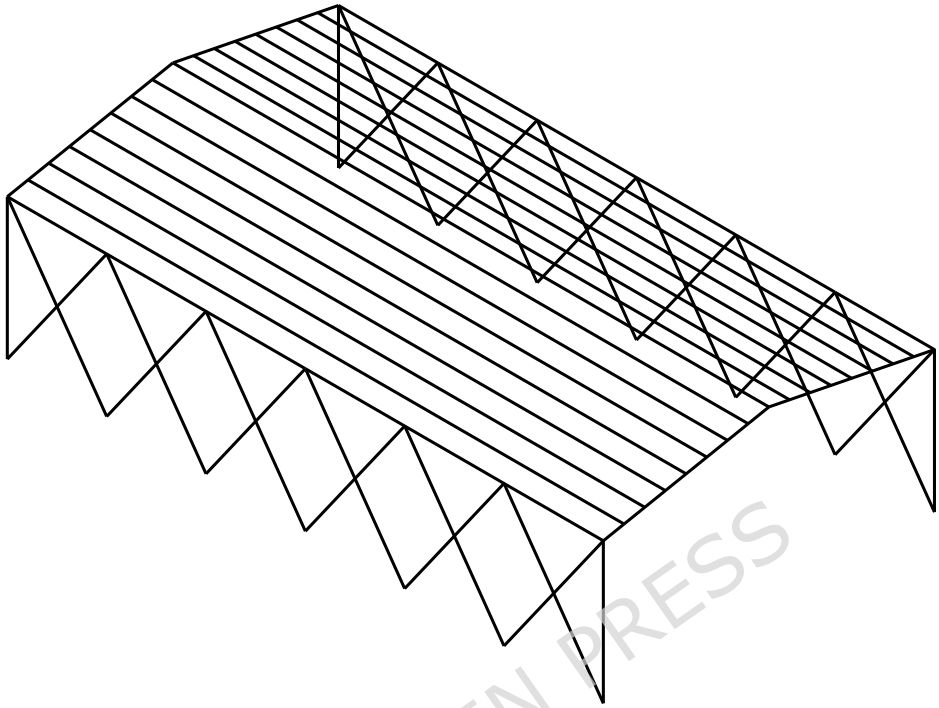

Figure 9. Building substructure

It is important to note that the nonlinear normal modes obtained for the substructure representing the remainder of the building do not include higher-order terms; therefore, they match the linear modes that would have been obtained from a damped modal analysis. This is because nonlinearities in the joints were only considered for the frames. The normal modes selected for model order reduction correspond to the horizontal displacements of the nodes connecting the previously described frames, along with the in-plane rotational modes. These modes are analogous to those employed in the computation of the nonlinear normal modes.

Furthermore, it is worth mentioning that the chosen substructuring strategy is not the only possible approach. However, as shown in Figures 7 and 8, the selected substructures have sufficient constraints to avoid being classified as free-floating [11]. This significantly simplified the solution process, since it eliminated the need to compute rigid body modes for each of these substructures. The displacement results for node *B* of the central frame can be seen in Figure 10.

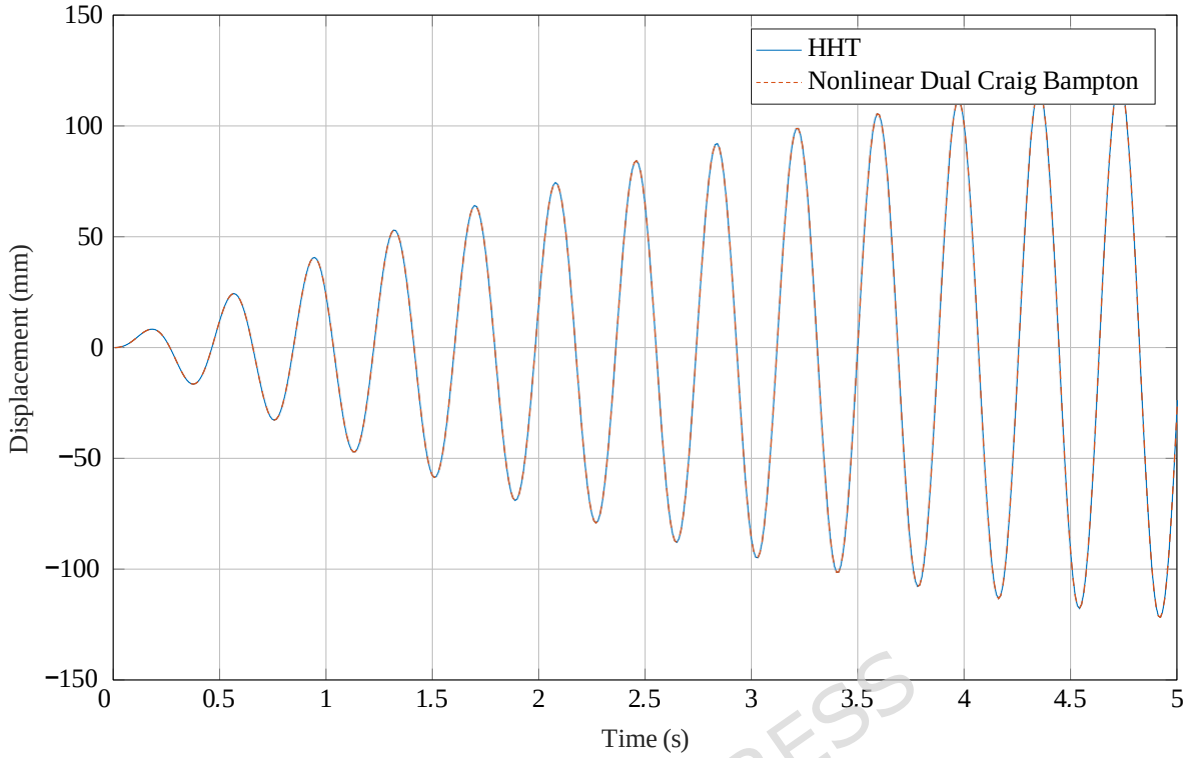

Figure 10. Horizontal displacement of node *B* of the central frame as a function of time in seconds using the proposed substructuring method

As observed, the displacement response curve of node *B* is almost entirely superimposed on the response obtained using the HHT method. Furthermore, by applying the HHT method to solve the system of equations resulting from the model order reduction, a simulation time of 94 s was achieved, using 75 MB of RAM. The example demonstrates the effectiveness of the method in determining the response of the industrial building, as the curves obtained from both approaches are closely aligned. Figure 11 presents the relative error between the two for selected time points, showing that these errors remain below values typically accepted in engineering practice. The relative error E is defined as:

$$\mathsf{E} = \frac{|v_{NLDCB} - v_{full}|}{|v_{full}|} \tag{27}$$

Where v_{NLDCB} is the displacement obtained with the proposed method and v_{full} is the displacement obtained by solving the full finite element model.

In this case, the reduction in computational time and resources required to determine the system response is not solely due to the decrease in the number of degrees of freedom, but also to the fact that it was only necessary to compute the nonlinear normal modes of two substructures: one frame and the rest of the building (as shown in Figures 7 and 8).

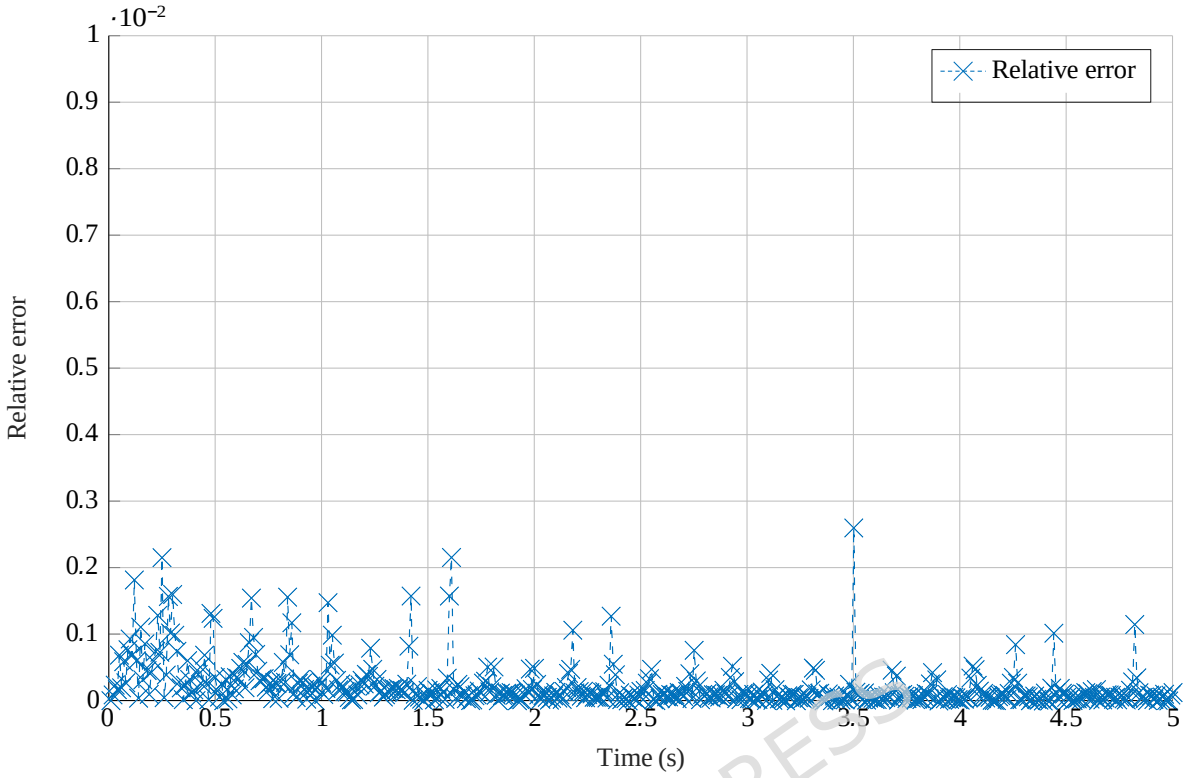

Figure 11. Relative error of the horizontal displacement at node *B* between the HHT method and the nonlinear dual Craig Bampton method

A convergence study was also performed, in which the maximum absolute error obtained during the simulation was compared against the number of nonlinear normal modes used in each substructure—particularly in each frame substructure. When a single nonlinear normal mode was used, it was based on the horizontal translation of node *B*; when two nonlinear normal modes were used, they were based on the horizontal translation and in-plane rotation of node *B*; when three nonlinear normal modes were used, they were based on the horizontal translation of nodes *B* and *D*, and the in-plane rotation of node *B*; and when four nonlinear normal modes were used, they were based on the horizontal translation and in-plane rotation of nodes *B* and *D*. The results of this study can be observed in Figure 12.

It was observed that the more nonlinear normal modes were selected, the smaller the absolute error obtained during the simulations became. However, it is important to note that when two nonlinear normal modes were chosen—one of which included the rotational degree of freedom—the relative error exhibited its most significant reduction. This occurs because selecting that particular nonlinear normal mode incorporated the degree of freedom directly affected by the cubic nonlinearity of the spring. This highlights the importance of selecting the appropriate degrees of freedom—those directly influenced by the inherent nonlinearities of the model—to achieve an accurate approximation of the results.

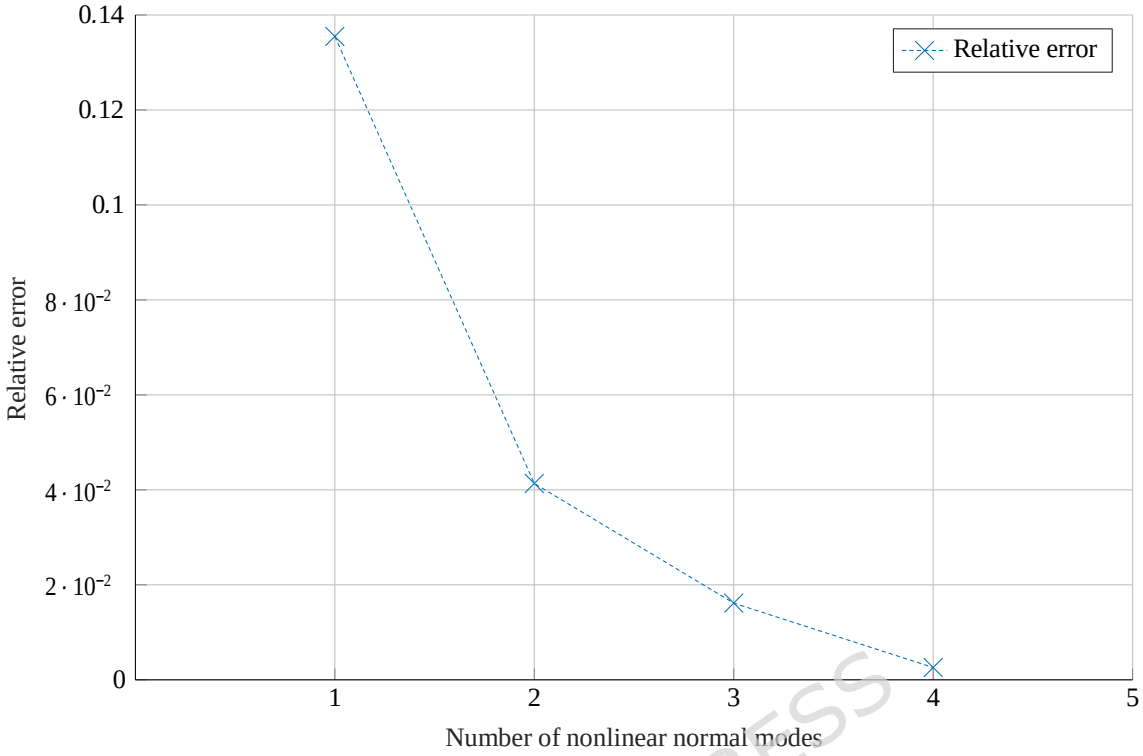

Figure 12. Maximum relative error found according to the number of nonlinear normal modes used in the simulation

3.2 Case study: Industrial building subjected to sinusoidal loads with non-proportional damping

The same industrial building considered in the previous case study was employed here, with the distinction that external body-to-ground dampers are introduced to intentionally produce a non-proportional damping matrix. The resulting damping contributions are localized at specific degrees of freedom and cannot be represented as a linear combination of the mass and stiffness matrices, thereby leading to non-proportional damping. The externally damped structure is shown in Fig 13.

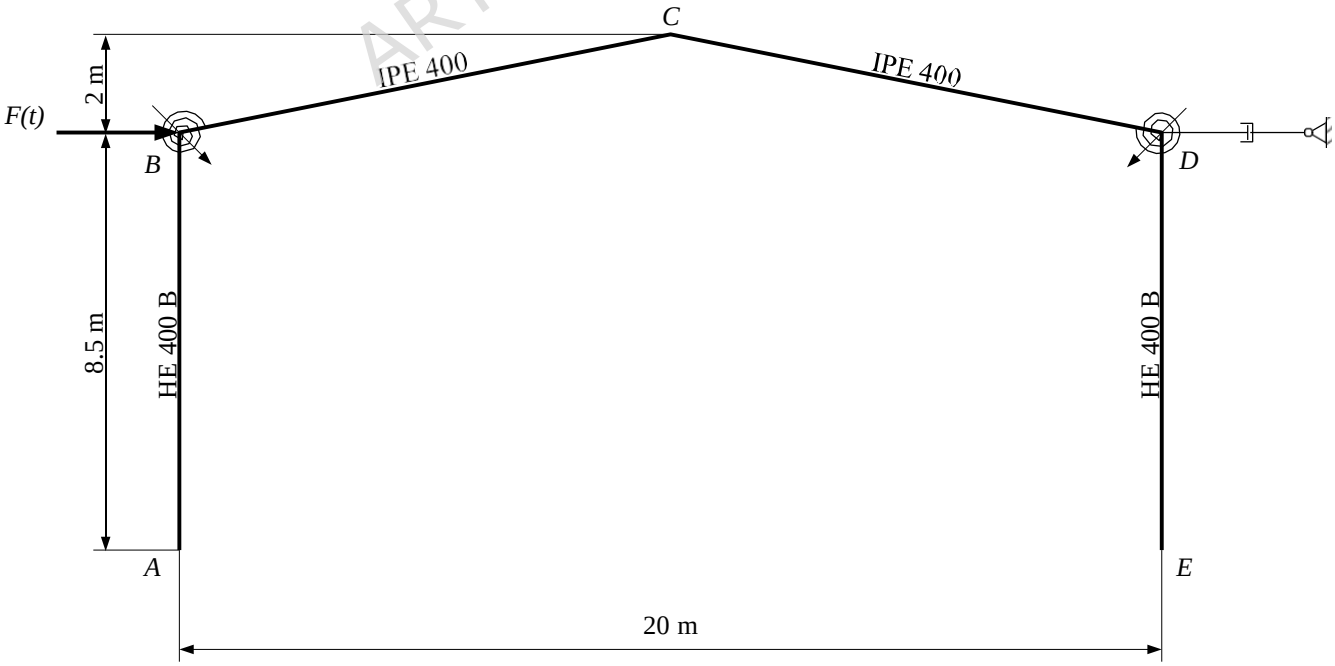

Figure 13. Building substructure with external dampers

3.2.1 Characteristics of the model

The same modeling characteristics as in the previous model were adopted; additionally, the force F_d exerted by the external dampers was assumed to follow the expression in Eq. 28.

$$F_d = c \cdot \dot{q} \tag{28}$$

Where c denotes the linear damping coefficient and $\dot{q}$ represents the velocity of the degree of freedom aligned with the damper direction. The characteristics of this model are presented in Table 3.

Table 3. Building Geometry, Material Properties, and Damping Coefficients

Characteristic	Magnitude	Unit
Column height	8.5	m
Span between columns	20	m
Total frame height	10.5	m
Spacing between frames	6	m
Density	7850	$kg \cdot m^{-3}$
Young's modulus	2.1×10^5	MPa
Poisson's ratio	0.3	
k	10	$N \cdot m^{-3}$
α	1.25×10^{-3}	s^{-1}
β	2.5×10^{-3}	s
c	2000	$N \cdot s \cdot m^{-1}$

3.2.2 Mesh

The same discretization used in the previous model was used for this case.

3.2.3 Loads and Boundary Conditions

The same loads and boundary conditions used in the previous model were used for this case.

3.2.4 Results using the HHT method

The equations of motion of the system are given by Eq. 26. The mass and stiffness matrices, **M** and **K**, remain unchanged, whereas the damping matrix **C** differs from that of the previous case due to the inclusion of the external dampers.

The initial time step for solving the equations of motion was set once again to $\Delta t = 0.01$ s, with the step size subsequently adjusted by ANSYS®'s built-in adaptive algorithm. The total simulation time required to solve the equations of motion, using the finite element discretization, was 381 s, and the process consumed 402 MB of RAM. Figure 14 presents the horizontal displacement of joint *B* in the central portal frame of the industrial building, obtained from a transient analysis performed with the HHT method.

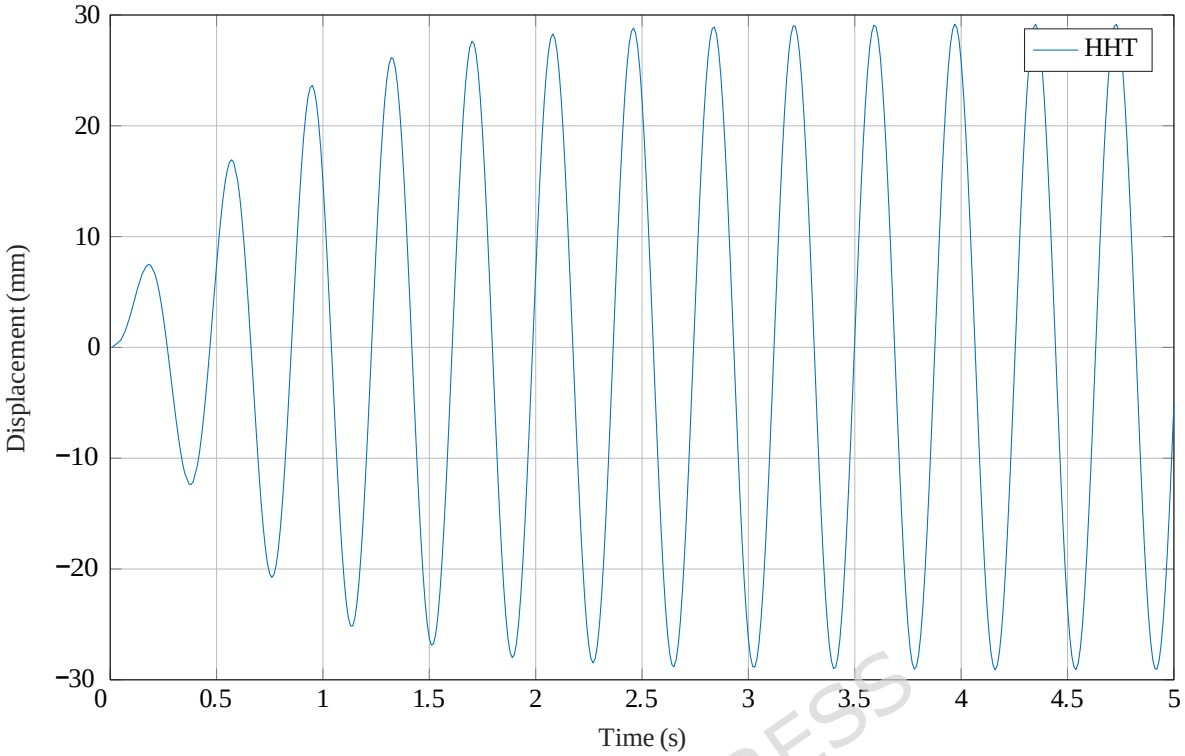

Figure 14. Horizontal displacement of node B of the central frame using HHT direct integration method

3.2.5 Results using the Implemented Substructuring method

The same substructuring strategy of the previous example was used for this case. The presence of an external damper in each substructure produces a non-proportional damping matrix for each one. Once again, the nonlinear normal modes were computed with respect to the translational and rotational degrees of freedom of nodes *B* and *D* in each substructure, and the state-space coordinates selected of the computation of the nonlinear normal modes were those corresponding to their horizontal displacements, as well as their in-plane rotations. The displacement results for node *B* of the central frame can be seen in Figure 15.

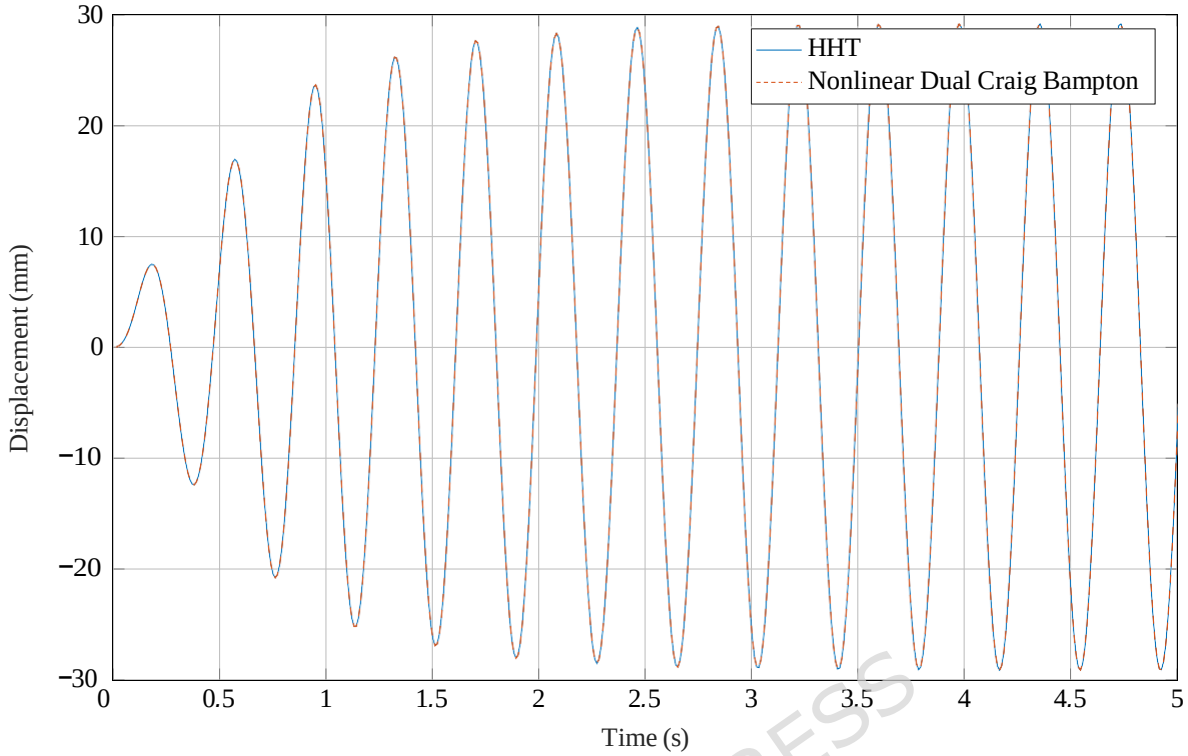

Figure 15. Horizontal displacement of node *B* of the central frame as a function of time in seconds using the proposed substructuring method

The displacement response curve of node *B* is observed once again to be closely aligned to the response obtained using the HHT method. By applying the HHT method to solve the system of equations resulting from the model order reduction, a simulation time of 102 s was achieved, using 76 MB of RAM. Figure 16 presents the relative error between both results, showing that these errors remain below values typically accepted in engineering practice.

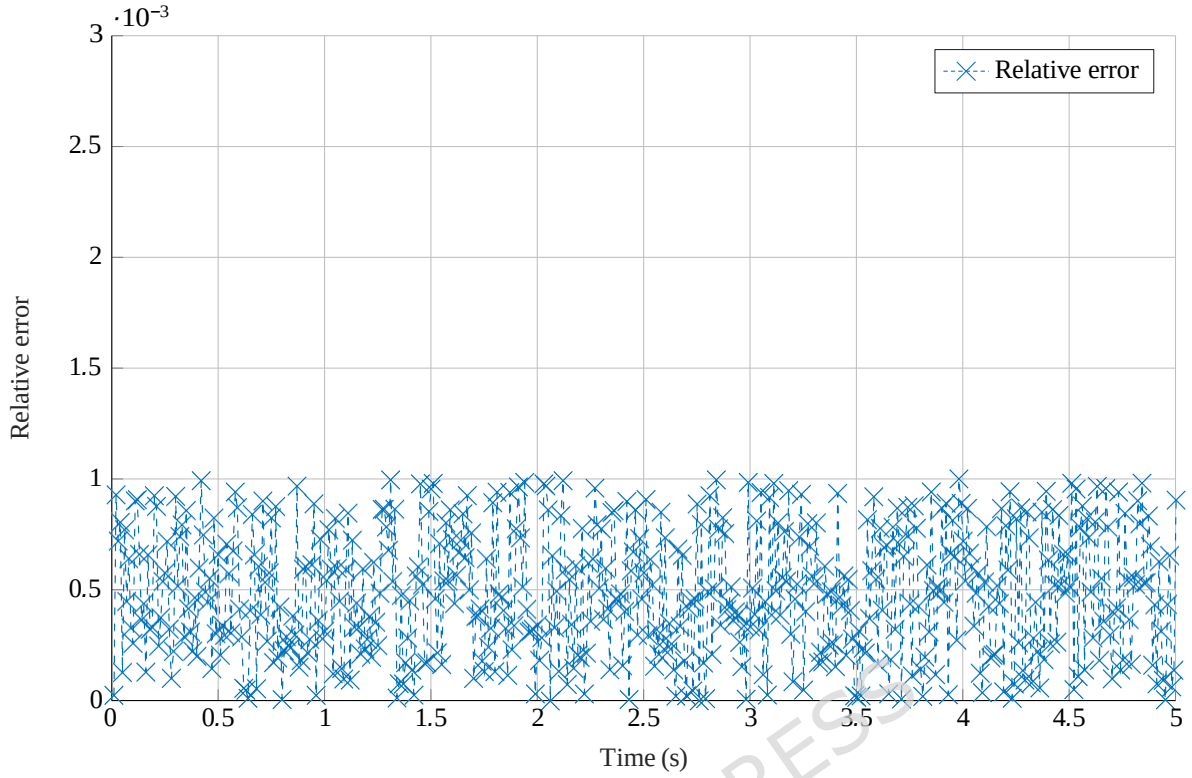

Figure 16. Horizontal displacement of node *B* of the central frame as a function of time in seconds using the proposed substructuring method

4 Conclusions

This research was conducted with the aim of introducing a novel substructuring method for the dynamic analysis of flexible body systems, particularly those exhibiting nonlinear behavior in their equations of motion. To achieve this, various solution strategies for nonlinear systems were explored within the framework of the finite element method. Among the approaches studied, the theory of nonlinear normal modes emerged as a promising alternative for reducing the order of nonlinear dynamic systems. This theory was integrated with the dual Craig Bampton method, originally proposed by [11] in its formulation that accommodates non-proportional damping in the equations of motion. In its original form, the dynamic approximation relied solely on conventional linear vibration modes; therefore, the primary modification developed in this work involved replacing them with nonlinear normal modes.

Through the examples proposed and developed in this study, it has been demonstrated that the proposed method effectively reduces both computational time and RAM usage compared to the iterative direct integration methods commonly employed for solving nonlinear systems. Furthermore, it has been confirmed that the accuracy of the system response remains within an acceptable margin.

As future work, it is proposed to implement this method in systems with a much larger number of degrees of freedom to assess its scalability and stability under different scenarios. The use of nonlinear normal modes for dynamic systems of this size has only recently begun to be explored by [16].

In addition, several methods for computing the nonlinear normal modes of a substructure are currently being developed or expanded ([16]; [27]), and it is expected that one of these approaches could serve as a foundation to further reduce the computational resources required. In the case study analyzed, only low-frequency excitation was considered, which limited the number of modes required to accurately represent the system dynamics. Consequently, the computational effort associated with computing the nonlinear normal mode coefficients was not significant. However, when analyzing higher excitation frequencies, a greater number of modes would be necessary to maintain accuracy, leading to increased computational cost. In such cases, the previously discussed methodologies for computing nonlinear normal modes could provide an effective means to mitigate

the associated computational burden.

On the other hand, [28] briefly suggested using nonlinear normal modes as a substructuring-compatible method. Future research could explore how to incorporate nonlinear normal mode theory into other substructuring approaches, particularly those that employ the state-space form of the equations of motion as part of the order reduction process, as was done in this work with the dual Craig Bampton method.

Finally, to refine the method proposed in this research, it is suggested to investigate how input conditions or loss of contact between two parts of a substructure (contact nonlinearity) can be integrated into the set of nonlinearities that this method is capable of handling. It is also recommended as future work to investigate the stability of the proposed method.

References

1. Guyan, R. J. Reduction of stiffness and mass matrices. *AAIA J.* **3**, 380 (1965).
2. Irons, B. Structural eigenvalue problems - elimination of unwanted variables. *AIAA J.* **3**, 961–962, DOI: 10.2514/3.3027 (1965).
3. Craig, R. & Bampton, M. Coupling of substructures for dynamic analyses. *AIAA Journal, Am. Inst. Aeronaut. Astronaut.* **6**, 1313–1319, DOI: 10.2514/3.4741Ã´r (1968).
4. Rubin, S. Improved component-mode representation for structural dynamic analysis. *AIAA J.* **13**, 995–1006, DOI: 10.2514/3.60497 (1975).
5. Yee-tak Leung, A. An accurate method of dynamic condensation in structural analysis. *INTERNATIONAL. JOURNAL FOR NUMERICAL METHODS IN ENGINEERING* **12**, 1705–1715 (1978).
6. Craig, R. R. & Chung, Y. T. Generalized substructure coupling procedure for damped systems. *AIAA J.* **20**, 442–444, DOI: 10.2514/3.51089 (1982).
7. Béliveau, J. G. & Soucy, Y. Damping synthesis using complex substructure modes and a hermitian system representation. *AIAA J.* **23**, 1952–1956, DOI: 10.2514/3.9201 (1985).
8. De Kraker, A. & Van Campen, D. H. Rubin's cms reduction method for general state-space models. *Comput. & Struct.* **58**, 597–606 (1994).
9. Cardona, A. Superelements modelling in flexible multibody dynamics. *Multibody Syst. Dyn.* **4**, 245–266, DOI: 10.1023/a:1009875930232 (2000).
10. Rixen, D. J. A dual craig-bampton method for dynamic substructuring. *J. Comput. Appl. Math.* **168**, 383–391, DOI: 10.1016/j.cam.2003.12.014 (2004).
11. Gruber, F. M. & Rixen, D. J. Dual craig-bampton component mode synthesis method for model order reduction of nonclassically damped linear systems. *Mech. Syst. Signal Process.* **111**, 678–698, DOI: 10.1016/j.ymssp.2018.04.019 (2018).
12. Rosenberg, R. The normal modes of nonlinear n-degree-of-freedom systems. *J. Appl. Mech.* **29**, 7–14, DOI: 10.1115/1.3636501Ã´r (1962).
13. Shaw, S. & Pierre, C. Normal modes for non-linear vibratory systems. *J. Sound Vib.* **164**, 85–124 (1993).
14. Haller, G. & Ponsioen, S. Nonlinear normal modes and spectral submanifolds: existence, uniqueness and use in model reduction. *Nonlinear Dyn.* **86**, 1493–1534, DOI: 10.1007/s11071-016-2974-z (2016).
15. Ponsioen, S., Jain, S. & Haller, G. Model reduction to spectral submanifolds and forced-response calculation in high-dimensional mechanical systems. *J. Sound Vib.* **488**, DOI: 10.1016/j.jsv.2020.115640 (2020).
16. Jain, S. & Haller, G. How to compute invariant manifolds and their reduced dynamics in high-dimensional finite element models. *Nonlinear Dyn.* **107**, 1417–1450, DOI: 10.1007/s11071-021-06957-4 (2022).
17. Apiwattanalunggarn, P., Shaw, S. W. & Pierre, C. Component mode synthesis using nonlinear normal modes. *Nonlinear Dyn.* **41**, 17–46, DOI: 10.1007/s11071-005-2791-2 (2005).

18. Huang, X. R., Jézéquel, L., Besset, S., Li, L. & Sauvage, O. Nonlinear modal synthesis for analyzing structures with a frictional interface using a generalized masing model. *J. Sound Vib.* **434**, 166–191, DOI: 10.1016/j.jsv.2018.07.027 (2018).

19. Xu, Z., Kaundinya, R. S., Jain, S. & Haller, G. Nonlinear model reduction to random spectral submanifolds in random vibrations. *J. Sound Vib.* **600**, DOI: 10.1016/j.jsv.2024.118923 (2025).

20. Zucca, S. On the dual craig–bampton method for the forced response of structures with contact interfaces. *Nonlinear Dyn.* **87**, 2445–2455, DOI: 10.1007/s11071-016-3202-6 (2017).

21. Latini, F., Brunetti, J., D'Ambrogio, W., Allen, M. S. & Fregolent, A. Nonlinear substructuring in the modal domain: numerical validation and experimental verification in presence of localized nonlinearities. *Nonlinear Dyn.* **104**, 1043–1067, DOI: 10.1007/s11071-021-06363-w (2021).

22. Soleimani, H. & Aage, N. Nonlinear dynamic substructuring in the frequency domain. *Comput. Methods Appl. Mech. Eng.* **439**, DOI: 10.1016/j.cma.2025.117882 (2025).

23. Kuether, R. J., Allen, M. S. & Hollkamp, J. J. Modal substructuring of geometrically nonlinear finite element models with interface reduction. *AIAA J.* **55**, 1695–1706, DOI: 10.2514/1.J055215 (2017).

24. Crisfield, M. *Non-linear Finite Element Analysis of Solids and Structures. Volume 1: Essentials*, vol. 1 (Wiley and Sons, 1991).

25. Crisfield, M. *Non-linear Finite Element Analysis of Solids and Structures. Volume 2: Advanced Topics*, vol. 2 (Wiley and Sons, 1991).

26. Hilber, H. M., Hughes, T. J. R. & Taylor, R. L. Algorithms in structural dynamics. *Earthq. Eng. Struct. Dyn.* **5**, 283–292 (1977).

27. Piqueira, J. R. C., Mazzilli, C. E. N., Pesce, C. P. & Franzini, G. R. *Lectures on Nonlinear Dynamics* (Springer Nature Switzerland, 2024).

28. Allen, M. S. *et al. Substructuring in Engineering Dynamics - Emerging Numerical and Experimental Techniques*, vol. 594 (Springer Nature Switzerland AG, 2020).

Author contributions statement

P.A.F. conceived the study, developed the method, conducted the simulations and validations, and wrote the first draft of the manuscript.

Additional information

Funding No funds, grants, or other support was received. **Employment** The author has no relevant employment interests to disclose **Financial and non-financial interests** The author has no relevant financial or non-financial interests to disclose.